Photochemistry and photophysics of novel photoinitiators: N,N,N-tributyl-N-(4-methylene-7-methoxycoumarin) ammonium borates

Ananda M. Sarker, Yuji Kaneko, Douglas C. Neckers *

Center for Photochemical Sciences, [1] *Bowling Green State University, Bowling Green, OH 43403, USA*

Abstract

The photochemistry and photophysics of N,N,N-tributyl-N-(4-methylene-7-methoxycoumarin) ammonium borates (1a–c) were investigated by steady state spectroscopy, laser flash photolysis and product analysis. Drastic solvent effects were observed in the absorption and emission spectra. These can be explained on the basis of intermolecular hydrogen bonding between borate complexes and the solvent molecules. The fluorescence quantum yield is quite low in benzene and increases with increasing solvent polarity. The main pathway for the formation of photoproducts was shown to involve electron transfer from the borate anion to the singlet excited states of the coumarin leading to efficient formation of the separated radical pair in acetonitrile. The rate constants for excited state quenching correlate with the free energy for electron transfer estimated from the oxidation potential of the borate anions. © 1998 Elsevier Science S.A. All rights reserved.

Keywords: Photoinitiators; Coumarin; Borate salts; Laser flash photolysis; Photoinduced electron transfer; Radical intermediates; Hydrogen bonding

1. Introduction

Since the report that triarylalkyl borate salts of cyanine dye could be used as visible light initiators for acrylate and methacrylate polymerization [1,2], considerable progress has been made in the use triarylalkyl borates in radiation curing [3–7]. The mechanism of radical chain initiation by the triphenylbutyl borate salts involves photoinduced electron transfer from the borate anion to an excited state of the chromophore, likely to form a triphenylbutyl radical, that in turn undergoes rapid C–B bond cleavage forming triphenyl boron and butyl radical. These butyl radicals have been shown to be the primary initiating species when triphenylbutyl borate salts are used [8].

In principle, tetraaryl borates can be used in place of triarylalkyl borates because the photoinduced electron transfer (PET) from the borate anion to the excited state of chromophore is, in general, thermodynamically more favorable due to the relatively low oxidation potential of the borates [9]. On the other hand, tetraarylborate salts have been thought to be inefficient coinitiators for radical polymeriza-

tion. However, there are some specific advantages in using tetraaryl borates since, in particular tetraphenyl borates, are more stable and easier to make than the corresponding triarylalkyl borates. Recently, we reported that tetraphenyl borate paired with cationic coumarin was as efficient photoinitiators of free radical polymerization as the corresponding triphenylbutyl borate, coumarin pair [10]. Owing to its extended absorption into the near UV–visible region, the activity of these compounds as visible photoinitiators would have important applications.

In this paper, we report photophysical and photochemical properties of the systems shown in Chart 1. Borates 1a and 1b contain the same light absorbing chromophore in the form of the cation and triphenyl borate or tetraphenyl borate as the counter anion. Borate 1c contained tetrafluoroborate, a non-oxidizable counter anion, and was used as a model compound wherein no electron transfer is expected.
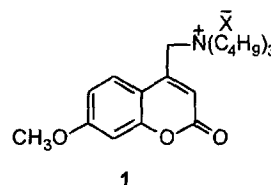
a. X = Ph$_3$BBu
b. X = Ph$_4$B
c. X = BF$_4$

1

2. Experimental

2.1. Materials

The synthesis of **1b–c** were described elsewhere [11]. Unless mentioned, all other compounds were obtained from Aldrich. 4-Bromomethyl-7-methoxycoumarin was recrystallized from ethanol prior to use. All spectroscopic grade solvents were purchased from Aldrich and used as received.

2.2. Instrumentation

Absorption spectra were recorded using a Hewlett Packard 8452A diode array UV–Vis spectrophotometer. Fluorescence spectroscopy was carried out using a SPEX Fluorolog spectrophotometer. Quantum yields of fluorescence were determined relative to 9,10-diphenylanthracene in hexane [12]. ^{1}H NMR spectra were taken on Gemini GEM-200 (200 MHz) spectrophotometer. GC-MS was performed on a Hewlett Packard 5988 mass spectrometer coupled to a HP 5880A GC, interfaced to a HP 2623A data processor. GC measurements were carried out on a Hewlett Packard (HP) 5890 gas chromatograph. Elemental analysis of new compounds was performed by Atlantic Microlab, GA.

All electrochemical experiments were conducted on a BAS-100 potentiostat with BAS PA-1 preamplifier. The reference electrode used was Ag/AgNO$_3$ with 0.1 M tetrabutylammonium perchlorate in acetonitrile solvent. The working electrode and counter electrode were platinum and a platinum wire, respectively. The rate of scan was adjusted to 200 mV s^{-1} in all experiments.

The nanosecond laser flash photolysis experiments employed a kinetic spectrophotometric detection system, which has been previously described [13]. The excitation source was the third harmonic from a Q-switched Nd:YAG laser (355 nm; 60 mJ/pulse; 8 ns pulse). However, only a small fraction of pulse energy was used in order to eliminate unnecessary processes. Transients produced were followed temporally and spectrally by a computer controlled kinetic spectrophotometer.

2.3. Preparation of N,N,N-tributyl-N-(4-methylene-7-methoxycoumarin) ammonium triphenylbutyl borate (1a)

To a solution of N,N,N-tributyl-N-(4-methylene-7-methoxycoumarin) ammonium bromide (0.77 g, 1.70 mmol) [11] in water (50 ml) was added slowly an aqueous lithium salt of triphenylbutyl borate^2 with stirring at room temperature. A slight stoichiometric excess of lithium salt of triphenylbutyl borate was used to ensure complete conversion. A white solid gradually precipitated, and the resulting mixture was stirred an additional 30 min. The solid was filtered, washed with water and then air dried overnight. After recrys-

tallization from ethanol, compound **1a** was obtained as white crystals (0.70 g, 61% yield); mp 66–67°C. ^{1}H NMR (acetonitrile): δ 7.71 (d, J = 9.8 Hz, 1H), 7.27 (m, 6H, ortho to B), 6.99 (m, 8H, meta to B and coumarin ring), 6.78 (t, J = 7.4 Hz, 3H, para to B), 6.37 (s, 1H), 4.41 (s, 2H), 3.90 (s, 3H), 3.20 (m, 6H), 1.93 (m, 2H), 1.86(m, 6H), 1.26 (m, 8H), 0.93 (m, 11H), 0.78 (t, J = 7.4 Hz, 3H). Anal. Calcd. for C$_{45}$H$_{60}$BNO$_3$: C, 80.27; H, 8.91; N, 2.08. Found: C, 80.39; H, 8.99; N, 2.08.

2.4. Irradiation of 1a–b in acetonitrile and characterization of the products

Compound **1a** or **1b** (0.75 g) was dissolved in 5 ml of dry degassed acetonitrile and placed in a Pyrex glass tube containing a magnetic bar. The sample was placed in a Rayonet reactor and irradiated at 300–400 nm for 1 h with stirring. One main photoproduct precipitated during the irradiation. It was filtered, washed with acetonitrile and characterized. The remaining solution was subjected to silica gel chromatography with hexane–ethyl acetate (9:1) as eluent and the following new products were characterized by ^{1}H NMR, mass spectroscopy and elemental analysis.

Di-(7-methoxy-4-coumarin) ethane **2**: mp > 300°C. MS m/z 378 (M$^+$), 377 (100%), 350, 226, 202, 190, 161, 137, 118, 89, 63. Anal. Calcd for C$_{22}$H$_{18}$O$_6$: C, 69.86; H, 4.76. Found: C, 69.97; H, 4.75.

4-Pentyl-7-methoxycoumarin **4**: ^{1}H NMR (CDCl$_3$): δ7.50 (d, J = 8.4 Hz, 1H), 6.84 (m, 2H), 6.14 (s, 1H), 3.88 (s, 3H), 2.51 (t, J = 7.0 Hz, 2H), 1.60 (m, 2H), 1.31 (m, 4H), 0.88 (t, J = 7.0 Hz, 3H). MS m/z 246 (M$^+$), 203 (100%), 175.

2.5. Quantum yield determination

In these experiments, 35 ml of a 3×10^{-4} M solution of **1a–b** in acetonitrile or benzene in a quartz cell (10 cm pathlength) was deoxygenated by purging with oxygen-free nitrogen for 30 min and sealed. Irradiation was performed using 366 nm light from a 200 W Hg lamp isolated from the spectrum with two color glass filters (cut off at 340 nm and at 400 nm). UV light was passed through a 10 cm water filter and focused into the sample. The maximum degree of photodecomposition was 20% in acetonitrile or benzene. The intensity of 366 nm light was determined using an anthracene dimerization reaction in oxygen free benzene (1.05×10^{-2} M, quantum yield of anthracene disappearance is 0.0706) [14]. The concentration of the remaining borates was determined by HPLC using methanol as eluent.

3. Results and discussion

3.1. Steady state spectroscopy

The absorption spectra of compounds **1a–c** are similar suggesting that the counter anions do not have much influ-

---

^{2} Lithium salt of triphenylbutyl borate was prepared by treating 1.6 M butyllithium in hexane with triphenyl boron in benzene at 10°C.

ence. However, the absorption maximum of 1a–c move toward the visible range (12 nm) without a change in the shape of the absorption as compared with 4-methyl-7-methoxycoumarin in acetonitrile. These results suggest that an interaction exists between the nitrogen cation and the boron anion in acetonitrile though there is no evidence for the formation of a ground state CT complex. This type of interaction has important consequences in both the kinetics and thermodynamics of electron transfer reactions. The absorption spectra of 1a at room temperature in different solvents $(1 \times 10^{-5}$ M) are shown in Fig. 1. In all solvents, abs spectra show a strong π,π^* transition in the region of 300–350 nm indicated by large molar absorption coefficients (Table 1).

No n,π^* transitions are observed because they are hidden under a strong π,π^* transition band [15,16]. However, solvent polarity has a significant effect on absorption spectra. The location of the absorption maximum is blue-shifted with increasing the polarity of the solvents. This solvent dependence phenomenon can be explained based on the energy of excited $^1\pi,\pi^*$ state and $^3n,\pi^*$ level of 1a associated with solvent polarity [17]. In nonpolar solvents the n,π^* singlet states are just above the $S_1(\pi,\pi^*)$ state, while n,π^* triplet states are below the $S_1(\pi-\pi^*)$ state [18]. In polar solvents, the energy of the $S_1(\pi-\pi^*)$ state is lowered below that of the n,π^* triplet state [18]. As a consequence, intersystem crossing from the $S_1(\pi,\pi^*)$ state to the closely lying $^3n,\pi^*$ state is efficient, and the fluorescence quantum yield is small. In polar solvents, quantum yield of fluorescence is higher due to inefficient intersystem crossing (Table 2 energy of the $S_1(\pi-\pi^*)$ state is below the $^3n,\pi^*$ state in the polar conditions.
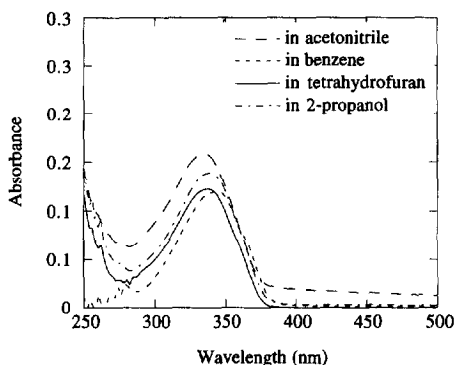

Fig. 1. Absorption spectra of 1a in different solvents at room temperature.

Table 1
UV–Vis absorption data of 1a in solvents of different polarity

Solvent	E [a]	λ_{max} (nm)	ε_{max} (M^{-1} cm^{-1})
Acetonitrile	35.94	334	14400
Isopropanol alcohol	19.92	338	13500
Tetrahydrofuran	7.58	339	12000
Benzene	2.28	344	11700

[a] Dielectric constant.

Table 2
Fluorescence emission and excitation data for 1a at room temperature

Solvents	λ_{max}^{em} (nm)	Φ_f	λ_{max}^{ex} (nm)	E_{st}^* (cm^{-1})
Acetonitrile	418	0.130	342	5316
Isopropanol alcohol	418	0.170	345	5062
Tetrahydrofuran	418	0.045	341	5402
Benzene	408, 431, 460	0.028	375	2157

*Stokes shift.

Fig. 2 shows fluorescence excitation spectra of 1a in several solvents. The effect of solvent polarity is more pronounced than that seen in the case of the absorption spectra. A large red-shift (about 50–60 nm) in the excitation maxima (around 375–400 nm) with respect to the longest λ_{max} of UV–visible absorption spectra is observed in nonpolar solvents such as benzene. However, this is insignificant in polar solvents. This unusual difference between the absorption and the excitation spectra in nonpolar solvents is uncommon. This is probably, as described before, due to very closely lying singlet and triplet states in nonpolar solvents. Intersystem crossing between two states may be faster than the internal conversion to the lowest singlet states. This may rise to the difference between absorption and excitation spectra, which is not important in polar environments.

Fluorescence emission spectra for 1a in different solvents at room temperature is basically the mirror image of the fluorescence excitation spectra (Fig. 3). As expected, the fluorescence quantum yield increases with the increasing solvent polarity (Table 2) due to reasons explained earlier. However, this solvent dependence fluorescence has also been explained [19] in terms of a 'proximity effect' that is the consequence of vibronic interaction between closely lying $^1\pi,\pi^*$ and $^1n,\pi^*$ states. Therefore, the fluorescence behavior in our system can also be accounted for in terms of the solvent dependent $^1\pi,\pi^*-^1n,\pi^*$ electronic energy gap.

An interesting observation is that both fluorescence emission and excitation in the nonpolar solvent (benzene) show vibrational structure with several peaks (Fig. 4), while in polar solvents (acetonitrile) the vibrational bands disappear and the spectra show structureless broad spectra. This sug-
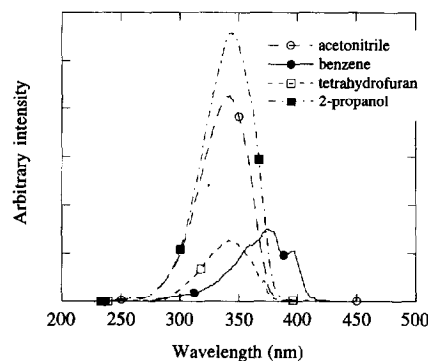

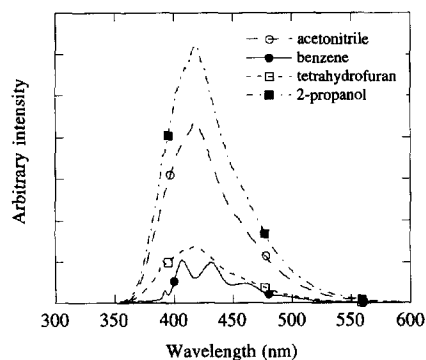Fig. 2. Fluorescence excitation spectra of 1a in different solvents.

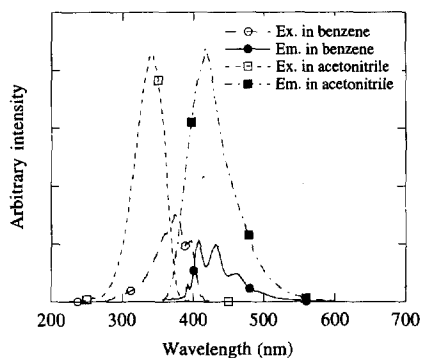Fig. 3. Fluorescence emission spectra of 1c in different solvents at room temperature.

Fig. 4. Fluorescence excitation and emission spectra of 1a in benzene and acetonitrile.

gests that the compound 1a interacts with acetonitrile or ethanol, probably through hydrogen bonding. This kind of interaction was also observed for simple coumarin derivatives [20,21].

3.2. Steady state photolysis

Irradiation of compound 1c at 350 nm in degassed anhydrous acetonitrile gave no reaction. On the contrary, com-

pounds 1a–b undergo chemical change under the same conditions and produce the products as shown in Scheme 1. Monitoring the photoreaction of 1a–b by ^{1}H NMR as a function of irradiation time revealed the continuous consumption of 1a–b and the formation of tertiary amine via C–N bond scission. ^{1}H NMR studies showed that approximately 1 h is enough for complete conversion (about 25 mg starting material) into amine. Conversion to amine was determined by observing the disappearance of the methylene peaks around 4.48 ppm and the appearance of a new peak at 2.43 ppm due to the formation of amine. Irradiation led to a precipitate of a white powder as a major product that does not dissolve in any common organic solvents. This colorless solid was identified through mass spectroscopy and elemental analysis as dimer 2. The remaining irradiated solution was analyzed by comparing GC-MS spectral patterns with authentic samples. The indicated products were identified.

When photolysis reactions were performed on a preparative scale, the yields of isolated products represent only lower limits but product distributions were similar in both small-scale and large-scale reactions (Table 3). The formation of tertiary amine and biphenyl in both reactions were in quantitative yields determined by ^{1}H NMR and GC, respectively. Identification of products 2, 3 and 4 clearly proves that radical 7-methoxy-4-methylenecoumarin 9, is the common intermediate for these products. The minor product 3 is formed in both cases via hydrogen abstraction from acetonitrile, a known hydrogen donor [22]. The mass spectrum of 3 obtained from deuterated acetonitrile exhibited a molecular ion peak 191 showing that the deuterium label had not been lost during the reaction and analysis. This confirms the hydrogen abstraction from solvents. The dimer 5 and the minor crossover product 4 indicate the presence of butyl radical that initiates the radical polymerization. There was no evidence that supported ionic intermediates of any kind.
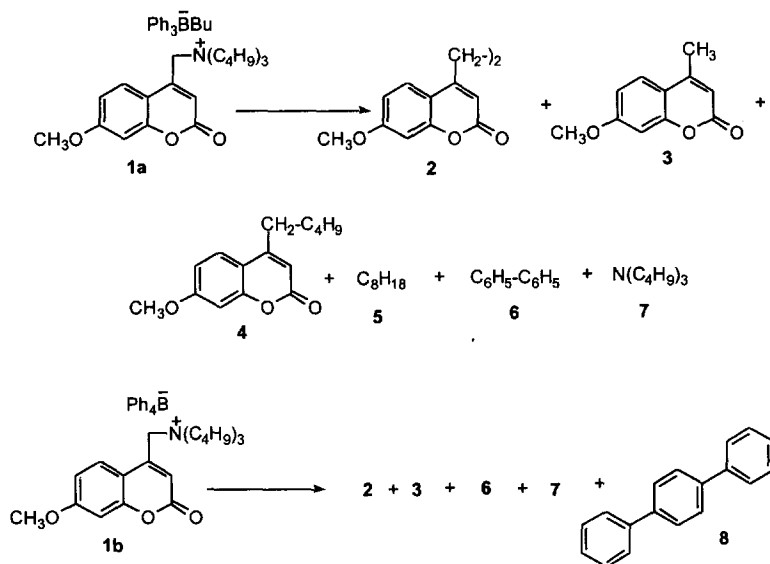
Scheme 1.

Table 3

Product studies for the photolysis of **1a–b** in acetonitrile for 1 h

Compounds [a]	Products (% yields)			
	2	3	4	8 [b]
1a	39	6	11	–
1b	42	10	–	5

[a] 100% conversion determined by TLC.
[b] Calculated by GC.

The formation of biphenyl as a coupling reaction of phenyl radicals is unlikely. Spin trapping experiments following electrochemical oxidation of Ph_4B^- anion failed to detect any phenyl radical even though the n-butyl radical was easily detected from a similar oxidation of tetra-n-butyl borate [23]. Labeling studies showed that two phenyl groups of the biphenyl come from the same borate, i.e., biphenyl is formed from carbons that were bound to boron [24,25]. Though the above experiments do not necessarily demonstrate the non-existence of phenyl radical in these systems, it is interesting to note that the both Ph_3BuB and Ph_4B boronyl radicals give almost an equal amount of biphenyl. Since the radical from Ph_3BuB dissociates in a few picoseconds to give triphenyl-boron and the butyl radical, it is reasonable to conclude that the biphenyl comes from triphenylboron. The only other possible fate of phenyl radical (if generated) would be conversion to benzene via hydrogen abstraction from acetonitrile. However, the detection of benzene in a reaction mixture in acetonitrile is virtually impossible.

Careful analysis of photoproducts for **1b** revealed the formation of terphenyl **8** in less than 10% (detected by GC-MS), while no indication is found for the same in **1a**. The terphenyl **8** is, however, probably produced from reaction between biphenyl and phenyl radical [26].

Acting on the assumption that the phenyl radical could not be generated, we rely only on the alternative pathway to explain the initiation of radical polymerization. One of the major photoproducts in our system is tertiary butyl amine. It is well known that an amine can generate an α-aminoalkyl radical via electron transfer to an acceptor containing carbonyl groups [27,28]. This α-amino alkyl radical is generated as a secondary photoproduct in the present system that is capable of initiating the polymerization of acrylates and methacrylates [29].

3.3. Laser flash photolysis

Laser flash photolysis of **1a** in degassed acetonitrile $(5 \times 10^{-4}$ M) leads to a transient with absorption bands at 480 and a broad band between 600–700 nm (Fig. 5). The lifetime of 480 nm transient is 1.5 μs with exponential decay. The broad absorption band (600–700 nm) decayed with second order kinetics $(k/\varepsilon = 1.3 \times 10^7$ cm s$^{-1})$. Both transient bands are quenched by addition of oxygen with different time profiles, indicating that the two species are independently
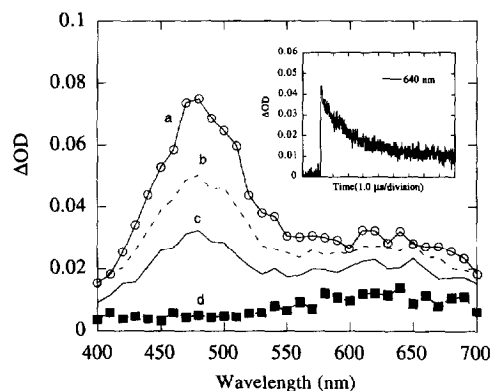

Fig. 5. Transient absorption spectra of **1a** $(5 \times 10^{-4}$ M) in acetonitrile recorded at (a) 0.59, (b) 1.2, (c) 1.8 and (d) 5.6 μs after irradiation. Inset: kinetic profile at 600 nm.
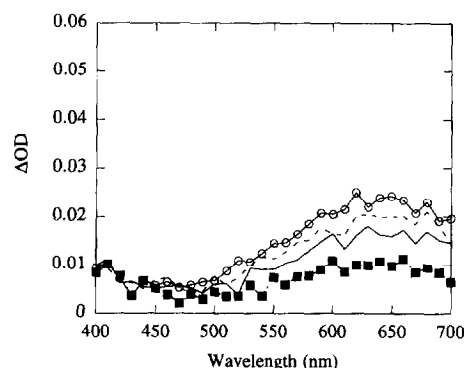

Fig. 6. Transient absorption spectra of 4-bromomethyl-7-methoxycoumarin in acetonitrile recorded at (a) 0.59, (b) 1.2, (c) 1.8 and (d) 5.6 μs after irradiation.

responsible for two absorption bands. The absorption at 480 nm is assigned to the triplet state of **1a** by comparison with the spectra generated from 4-methyl-7-methoxycoumarin in benzene $(\tau = 1.2$ μs, $\lambda_{max} = 470$ nm). A similar triplet transient was observed when **1c** $(1 \times 10^{-4}$ M) is photolysized under identical conditions, where BF_4 (no oxidizable) as counter anion. This triplet state at 480 nm was not quenched by addition of donors Ph_4B^-,Bu_4N^+ or Ph_3BuB^-,Bu_4N^+ $(2 \times 10^{-3}$ M in acetonitrile). Instead, a new broad absorption at 600–700 nm appeared with decay behavior similar to **1a** (at 640 nm). This broad 600–700 nm band is assigned to the radical **9**. This assignment was further confirmed by comparison with separately generated radical from 4-bromomethyl-7-methoxycoumarin (Fig. 6).

3.4. Electron transfer studies

3.4.1. Fluorescence quenching

Since the triplet state of **1c** is not quenched by donors such as Ph_3BuB^-, Bu_4N^+ and Ph_4B^- Bu_4N^+, we have performed fluorescence quenching experiments and found that the borates did quench the fluorescence of **1c** in acetonitrile very efficiently. If a charge transfer (CT) complex forms from **1c**, then fluorescence quenching may involve both static and dynamic mechanisms. In order to see whether any CT com-

plex has formed, the absorption spectra of 1c was studied in the presence of the borate donors of various concentrations. We did not observe any CT complex formation in acetonitrile solutions.

Using these borate donors as the quencher, plots of the fluorescence intensity vs. quencher concentration [Q] fitted the Stern–Volmer equation

$$I_0/I = I + k_q \tau_s [Q]$$

where k_q is the quenching rate constant and τ_s is the singlet state life time.[3] The quenching rates obtained exceeded the diffusion controlled limit (Table 4). The linear Stern–Volmer quenching plots (Fig. 7) indicate that only dynamic quenching is taking place in the concentration range studied. The rate constants for excited state quenching correlate with the free energy for electron transfer estimated and the oxidation potential of the donors.

3.4.2. Electrochemical studies

The fluorescence quenching of 1c with borate donors occurs by electron transfer from borate anions to the excited singlet state of 1c. In order to estimate the free energy change ($\Delta G°$) associated with this electron transfer reaction, we have measured the reduction potential of 1c in acetonitrile using cyclic voltammetry. The cyclic voltammetry measurement yielded a wave characteristic of irreversible one electron reduction with peak − 1.30 V vs. SCE (Fig. 8) as reduction potential. The absence of the reverse anodic peak in the cyclic voltammogram is reported for other dissociative systems [11]. The absence of reversible anodic peak suggests that the rapid and irreversible bond cleavage reaction occurs after reduction.

The oxidation potentials of Ph_4B^-,Bu_4N^+ and Ph_3BuB^-,Bu_4N^+ are known to be 0.90 V and 0.70 V, respectively [31]. Using the redox potential of 1c, the free energy change for electron transfer can be estimated by the Weller equation [32]. The $\Delta G°$ values are − 1.13 and − 1.33 eV for donors Ph_4B^-,Bu_4N^+ and Ph_3BuB^-,Bu_4N^+, thus indicating that the electron transfer is a highly exothermic process. The singlet state energy for 1c is calculated as 3.33 eV in acetonitrile (cross-point between fluorescence emission and excitation spectra).

3.5. Quantum yields for disappearance

The quantum yield for disappearance of 1a (4.12×10^{-4} M) and 1b (4.78×10^{-4} M) in benzene were determined with 366 nm light as excitation. To ensure complete absorbance of the incident light, a quartz cell having a path length of 10 cm was used. The quantum yield Φ_d of 1a and 1b are 0.39 and 0.20, respectively in benzene at above concentrations. In acetonitrile solution, photodecomposition of 1a (5.12×10^{-3} M) and 1b (5×10^{-3} M) were found to pro-

---

[3] τ_s is calculated as 34 ps using $\Phi_f = 0.13$ for 1a (see Table 4 in text) and $\tau_f = 0.23$ ns for 4-methyl-7-methoxycoumarin in methanol (see Ref. [30]).

Table 4
Quenching constants and free energy changes of 1c with borates

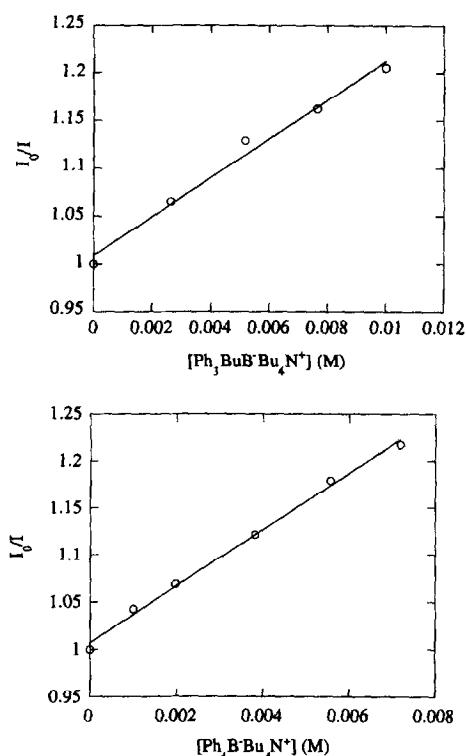| Borate anions	E^{ox} (V) vs. SCE	$\Delta G°$ (eV)	k_q (M^{-1} s^{-1})
Ph$_3$BBu	0.70	− 1.33	8.72×10^{11}
Ph$_4$B	0.90	− 1.13	5.82×10^{11}

Fig. 7. Stern–Volmer plots of 1c with tetrabutylammonium triphenylbutyl (above) and tetrabutylammonium tetraphenyl (below) borate.
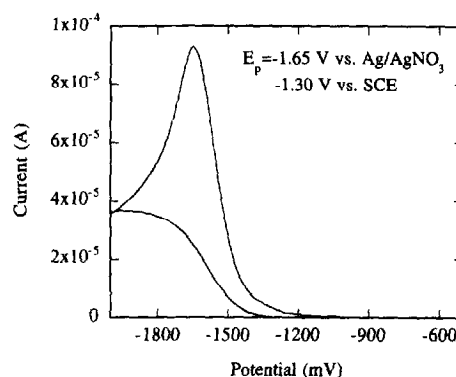

Fig. 8. Cyclic voltammogram of 1c in acetonitrile.

ceed with 0.17 and 0.07, respectively. In acetonitrile, the borate complex exists in a state of ionic equilibrium, thus diffusion of the ions is required for the ET reaction to take place. In benzene however, the borate exists as a tight ion pair, thus eliminating the diffusion controlled step and increasing the Φ_d.

3.6. Electron transfer mechanism

On the basis of the above observations, we have concluded that electron transfer is the primary photochemical step. The overall reaction mechanism we suggest is shown in Scheme 2. The singlet excited state of coumarin is involved and directly oxidizes the borates, as shown by the negative calculated $\Delta G°$ and measured fluorescence quenching (Table 4, notice that no ground state CT complex is formed, or at least none revealed by UV–Vis spectroscopy). The time resolved results and product studies are consistent with the assignment of the transient intermediate absorbing with a maxima at 600–700 nm to a radical 9. Scheme 2 shows the mechanism for the photoreduction of borate 1a. The same mechanism pertains for the compound 1b. Electron transfer from the borate anion to the excited coumarin moiety gives the radical 10 and the boranyl radical both of which dissociate rapidly. The lifetime of triphenylbutyl boranyl radical is 250 fs [9] and it dissociates to give a butyl radical that initiates polymerization. Back electron transfer is virtually impossible in such a short lifetime period. On the other hand, we are unable to detect the radical 10 from 1a or 1b using picosecond flash photolysis. An absorption growth for radical 9 is observed in both cases during the picosecond laser pulse indicating a unimolecular formation process. The C–N bond breaking process leading to the formation of radical 9 is coupled to the primary electron transfer process occurring on the sub-picosecond time scale. Back electron transfer in the case of tetraphenyl boranyl radical is again impossible with this time scale, although its life time is 45 ps [9]. At this point we argue that the formation of radical 9 follows either a or b.

In general, the borate salt exists as a contact ion pair in nonpolar solvents and as a solvent separated ion pair in polar solvents [2]. However, spectroscopic observation reveals that the borates 1a–b in acetonitrile have significant interaction between ion pairs than is expected of solvent separated ion pair. Hence, the quenching process is, in principle, very close to being intramolecular in acetonitrile.

The quenching process exceeded the diffusion controlled rate for both borate donors (Table 4). It is well known that the Stern–Volmer equation is not valid if the rate constant of the observed quenching process approaches or exceeds the diffusional limit, and the intermediate involved is very short lived [33,34]. Due to this effect, it is difficult to discuss these values, but they seem to correlate in a similar manner with the difference of oxidation potential of the borates. It should be mentioned that a high rate constant for excited state quenching does not necessarily equal a high efficiency for disappearance of starting materials [35]. Preliminary experiments have shown the relatively low quantum yield of disappearance of 1a and 1b in acetonitrile. Given that singlet states are responsible for photodissociation, the low quantum yields for dissociation is probably due to short lifetime as well as the presence of other deactivation processes. The quantum efficiencies would also be determined by the competition among three process in the initially formed radical pair (10 and triphenylbutyl boronyl). They are back electron transfer, radical pair separation and bond fragmentation. However, in the present system where both oxidative and reductive cleavage take place in very short time, radical pair separation can no longer operate. Therefore, we suggest that the difference of quantum yields for disappearance of 1a and 1b are due to the rate of C–B bond fragmentation (lifetimes of triphenylbutyl vs. tetraphenyl boronyl radicals) as well as oxidation potentials of borate anions.

4. Conclusions

The photochemistry of a new class of photoinitiators based on tetraorganyl borate salts has been presented. Self-destructive cationic coumarin is a powerful electron acceptor, and therefore efficiently oxidizes borate anions. Since the photoinduced electron transfer leads to rapid fragmentation, the electron transfer is driven in one direction. The efficiency of polymerization is determined by the rapid radical release from the system. With a suitable choice of the components based on electrochemical and thermodyamic properties, new borate photoinitiators can be designed, no matter whether triphenylbutyl or tetraphenyl borate anion is used.

Photogenerated tertiary amines in the present system are acting as synergists, but they also have another very important

Scheme 2.
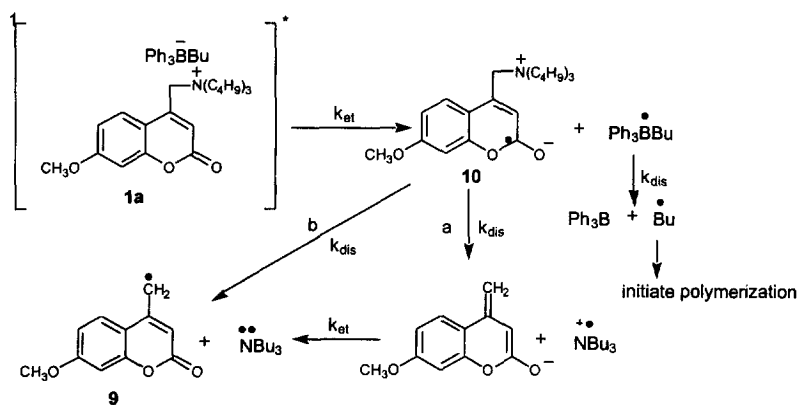
role. Free radical initiated polymerization reactions suffer from oxygen inhibition, i.e., the photogenerated radicals and the growing macroradicals are scavenged by oxygen. The presence of amines in the polymerization media helps to ameliorate the situation [36,37]. Besides this, the photogeneration of tertiary amines from soluble organic precursors is a field of increasing interest, especially in polymer curing and imaging process [38,39]. Of particular interest is the case of epoxide cross-linkage reactions where tertiary amines act as photoinitiators and create photoimaging system [40].

Acknowledgements

References

[1] S. Chatterjee, P. Gottschalk, P.D. Davis, G.B. Schuster, J. Am. Chem. Soc. 110 (1988) 2326.

[2] S. Chatterjee, P.D. Davis, P. Gottschalk, M.E. Kurtz, B. Sauerwien, X. Yang, G.B. Schuster, J. Am. Chem. Soc. 112 (1990) 6329.

[3] P. Gottschalk, D.C. Neckers, G.B. Schuster, U.S. Patent 4842980, 1989.

[4] P. Gottschalk, U.S. Patent 4874450, 1989.

[5] K. Kawamura, Y. Okamoto, U.S. Patent 4971891, 1990.

[6] M. Koike, N. Kita, U.S. Patent 4950581, 1990.

[7] P. Gottschalk, D.C. Neckers, G.B. Schuster, U.S. Patent 5051520, 1992.

[8] A.M. Sarker, A. Lungu, D.C. Neckers, Macromolecules 29 (1996) 8047.

[9] S.T. Murphy, C. Zou, J.B. Miers, R. Ballew, D. Dlott, G.B. Schuster, J. Phys. Chem. 97 (1993) 13152.

[10] R. Popielarz, A.M. Sarker, D.C. Neckers, Macromolecules 31 (1998) 951.

[11] A.M. Sarker, Y. Kaneko, A.V. Nikolaitchik, D.C. Neckers, J. Phys. Chem., 102 (1998) 5375.

[12] S. Hamai, F. Hirayama, J. Phys. Chem. 87 (1983) 83.

[13] W.E. Ford, M.A.J. Rodgers, J. Phys. Chem. 98 (1994) 3822.

[14] N.C. Yang, D.M. Shold, B. Kim, J. Am. Chem. Soc. 98 (1976) 6587.

[15] R.H. Abu-Eittah, B.A.H. EJ-Tawil, Can. J. Chem. 63 (1985) 1173.

[16] A.D.S. Marques, G.S.S. Marques, Photochem. Photobiol. 59 (1994) 153.

[17] K. Muthukamu, V. Ramamurthy, J. Photochem. 26 (1984) 57.

[18] G. Wenska, S. Paszyc, Can. J. Chem. 66 (1988) 513.

[19] T.I. Lai, B.T. Lim, E.C. Lim, J. Am. Chem. Soc. 104 (1982) 7631.

[20] J.B. Gallivan, Mol. Photochem. 2 (1970) 191.

[21] W.W. Mantulin, P.-S. Song, J. Am. Chem. Soc. 95 (1973) 5122.

[22] M.A. Ratcliff, J.K. Kochi, J. Org. Chem. 36 (1971) 3112.

[23] E.E. Bancroft, H.N. Blount, E.G. Janzen, J. Am. Chem. Soc. 101 (1979) 3692.

[24] D.H. Geske, J. Phys. Chem. 66 (1962) 1743.

[25] J.D. Wilkey, G.B. Schuster, J. Org. Chem. 52 (1987) 2117.

[26] J.C. Scaiano, L.C. Stewart, J. Am. Chem. Soc. 105 (1983) 3609.

[27] J.E. Christensen, W.L. Wooten, P.J. Whitman, J. Radiat. Cur. 14 (1987) 35.

[28] C.R. Morgan, D.R. Kyle, J. Radiat. Cur. 10 (1983) 4.

[29] H.J. Hagemann, Photopolymerization and Photoimaging Science and Technology, Chap. 1, Elsevier, London, 1989.

[30] J.R. Heldt, J. Heldt, M. Ston, H.A. Diehl, Spectrachim. Acta Part A 51 (1995) 1549.

[31] G.B. Schuster, Pure Appl. Chem. 62 (1990) 1565.

[32] D. Rehm, A. Weller, Isr. J. Chem. 8 (1970) 259.

[33] J. Keizer, J. Am. Chem. Soc. 105 (1983) 1494.

[34] R.M. Noyes, Prog. React. Kinet. 1 (1961) 131.

[35] G. Pohlers, J.C. Scaiano, R. Sinata, R. Brainard, D. Pai, Chem. Mater. 9 (1997) 1353.

[36] G. Bradely, R.S. Davidson, Recl. Trav. Chim. Pays-Bas 114 (1995) 528.

[37] G.J. Jiang, Y. Shirota, H. Mikawa, Polym. Photochem. 7 (1986) 311.

[38] J.M.J. Frechet, Pure Appl. Chem. 64 (1992) 1239.

[39] A.M. Sarker, A. Mejiritski, B.R. Wheaton, D.C. Neckers, Macromolecules 30 (1997) 2268.

[40] A. Mejiritski, A.M. Sarker, B.R. Wheaton, D.C. Neckers, Chem. Mater. 9 (1997) 1488.